ACS APPLIED MATERIALS & INTERFACES

RESEARCH ARTICLE

www.acsami.org

Impurity-Dependent Photoresponse Properties in Single CdSe Nanobelt Photodetectors

Peicai Wu, Yu Dai, Tuo Sun, Yu Ye, Hu Meng, Xiaolong Fang, Bin Yu, and Lun Dai*

State Key Lab for Mesoscopic Physics and School of Physics, Peking University, Beijing 100871, China

ABSTRACT: Impurity-dependent photoresponse properties of semiconductor nanostructures are studied for the first time in the photodetectors (PDs) made from intrinsic (*i*-) and extrinsic *n*-type single CdSe nanobelts (NBs). Both ohmic and Schottky contact based CdSe NB PDs were studied. The sizes of *i*- and *n*-NBs were purposely chosen to be nearly identical to minimize the size-dependent effect. Our experimental results demonstrate that *i*-CdSe NBs are more suitable for fast and sensitive PD applications, while *n*-CdSe NBs are more advantageous for high-gain PD applications. The different photoresponse properties result mainly from the impurity induced traps inside the CdSe NBs. This conclusion can be applicable to other semiconductor nanomaterials. Moreover, we have achieved short response/recovery times (~15/31 μs) and a high photosensitivity (~100) simultaneously from the *i*-CdSe NB PDs under a 3500 Hz pulsed illumination. This may be the best reported result so far in the effort of getting fast speed and high photosensitivity simultaneously from nanostructure based PDs for practical applications.

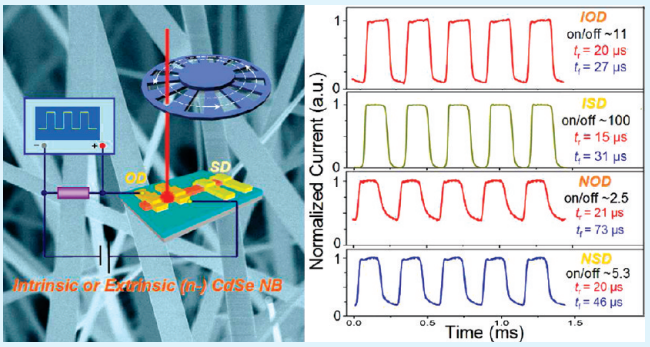

KEYWORDS: impurity, photodetector, photoresponse, CdSe, nanobelt, nanostructure

INTRODUCTION

As one of the most important applications of semiconductor materials, photodetectors (PDs), which convert optical signals into electrical signals, are essential elements in many fields, such as imaging techniques, optical communications, as well as in future memory storage, and intrachip optical interconnects, etc.[1−9] PDs of high photosensitivity, fast speed, high gain, and small device size are highly desired for practical applications.[10−13] Compared with their bulk counterparts, semiconductor nanostructures (NSs) have the advantage of higher photosensitivity because of their high surface-to-volume ratio. Moreover, the reduced dimension of the effective conductive channel shortens the carrier transit time, which would bring on both faster speed and higher gain.[6−9] Up to date, various semiconductor NSs, such as nanowires (NWs), nanotubes, and nanobelts (NBs), have been investigated for photoconductive characteristics.[14−28] The mechanisms of carrier photogeneration, transport, and collection in semiconductor NS PDs have been addressed in a number of studies. Based on the previous reports, there are mainly three dominating optoelectronic processes in semiconductor NS PDs: (1) photodoping effect resulted from the uprising of quasi-Fermi level of the carriers caused by photogenerated excess carriers, which leads to the increase in conductivity;[6,15,26] (2) photoconductance effect arised from band bending caused by surface electric field at NS surface.[4,18,29] Specifically, in some noble metal nanoparticles decorated nanomaterials, the enhanced space charge effect via the formation of localized Schottky junctions at the surfaces of the nanomaterials can result in a more pronounced electron−hole separation effect.[16,30] 3) photogating effect caused by trapping of photogenerated excess minority carriers, which would prolong the photocarrier lifetime.[6,7,15] Gas molecules adsorption/desorption at the NS surfaces would enlarge this effect in some cases.[7] Moreover, the contact types between semiconductor and metal electrodes are demonstrated to have great influence on the performance of the PDs. Good ohmic contact-based PDs tend to achieve higher gain, while Schottky contact based PDs usually exhibit higher photosensitivity and faster speed compared with ohmic contact-based PDs.[11−13]

Despite the abundant reports on the photoresponse properties of the semiconductor NS based PDs, to the best of our knowledge, the impurity-dependent photoresponse properties of them have received little attention and are not well understood. The impurities in semiconductor will affect the carrier concentration which determines the Fermi level. Accordingly, they will affect the contact type between semiconductor and the metal electrodes, and hence, affect the charge transport and collection of a PD. They will also affect the carrier lifetime and mobility in semiconductor. Moreover, the impurities can bring on the traps and defect states, which play an important role in the photoresponse properties of semiconductor NS PDs.[7,15] Thereby, the photoresponse properties of semiconductor NSs must be impurity dependent. In this work, we experimentally demonstrate the impurity-dependent photoresponse properties for the first time by studying the PDs made from intrinsic (*i*-) and extrinsic *n*-type CdSe NBs. Particularly, we employed two In/Au ohmic

Received: January 13, 2011
Accepted: May 2, 2011
Published: May 02, 2011

electrodes and two Ni/Au Schottky electrodes on single *i*- and *n*-CdSe NBs, thus four types of PDs were fabricated and studied simultaneously. Our experimental results together with the analysis demonstrate that intrinsic semiconductor NSs are more suitable for fast and sensitive PD applications, while extrinsic semiconductor NSs are more advantageous for high-gain PD applications. The different photoresponse properties of the CdSe NBs result mainly from the impurity induced traps inside the NBs. This conclusion can be applicable to other semiconductor nanomaterials. Moreover, our results also support the conclusion that Schottky contact based PDs show faster speed and higher photosensitivity, whereas the ohmic contact based PDs possess higher gain.[11−13] Particularly, the Schottky contact based *i*-CdSe NB PDs can perform fast speed (~15 μs) and high photosensitivity (~100), which may be the best reported result so far in the effort of getting a fast speed and a high photosensitivity, simultaneously, in NS-based PDs.[31]

EXPERIMENTAL SECTION

Synthesis and Characterization of CdSe NBs. The *n*-type CdSe NBs were synthesized via an atmospheric chemical vapor deposition (CVD) method in a tube furnace.[32] CdSe powder (99.995%) placing at the upstream of Ar carrier gas was used as the source. Pieces of Si wafers covered with 10 nm thick thermally evaporated Au films were used as substrates. A tiny Cd grain (99.95%) was placed between the source and the substrates as the dopant. The temperatures at the source and substrates were about 870 and 650−750 °C, respectively. The as-synthesized CdSe NBs exhibited *n*-type conductivity due to selenium vacancies and/or cadmium interstitials, which served as shallow donors in CdSe. Intrinsic CdSe NBs were synthesized in a process similar to the above one, except that no Cd dopant was introduced. The sythesized CdSe NBs were characterized by a field emission scanning electron microscope (FESEM; Amray 1910 FE) and a high-resolution transmission electron microscope (HRTEM; Tecnai F20). The photoluminescence (PL) measurement of the CdSe NBs was done with a microzone confocal Raman spectroscope (HORIBA Jobin Yvon, LabRam HR 800) equipped with a charge coupled device (CCD). The 325 nm line of a He−Cr laser was used as the excitation source.

Fabrication and Measurements of Single CdSe NB Photodetectors. First, the CdSe NB suspension was dropped on an oxidized Si substrate with a 500 nm SiO_2 layer. Then, UV lithography, followed by thermal evaporation and lift-off process, was used to fabricate two Schottky contact Ni/Au electrodes (20/150 nm) on an individual *i*- (*n*-) CdSe NB. Finally, two ohmic contact In/Au electrodes (20/150 nm) were fabricated on the same *i*- (*n*-) CdSe NB away from the two Ni/Au electrodes by the similar process as mentioned above. The spaces between the two Ni/Au electrodes and two In/Au electrodes were both about 2.5 μm. It is worth noting that the sizes of the *i*- and *n*-CdSe NBs used here were purposely chosen to be nearly identical in order to minimize the size-dependent effect.[4,33] For clarity, the *i*- and *n*-CdSe NB PDs with two Schottky contacts are labeled as ISD and NSD, whereas those with two ohmic contacts are labeled as IOD and NOD, respectively. The room-temperature electrical transport measurements were conducted with a semiconductor characterization system (Keithley 4200) in air. To measure the high-speed photoresponse properties, a mechanical light chopper (SRS SR540) was used to turn the 633 nm He−Ne laser, and an oscilloscope (Tektronix DPO2024) was used to monitor the time dependence of the photocurrent.

RESULTS AND DISCUSSION

The morphologies, crystal structures, and PL spectra of the synthesized *i*- and *n*-CdSe NBs are similar. Figure 1a shows a typical FESEM image of the CdSe NBs. Each CdSe NB has a smooth surface and a uniform width along the growth direction. The NBs are usually tens to hundreds of micrometers in length, submicrometer to several micrometers in width, and 50−100 nm in thickness. Figure 1b shows a typical HRTEM image and the corresponding selected area electron diffraction (SAED) of a CdSe NB, which reveal that the CdSe NB is a high-quality single crystal with the hexagonal structure. The CdSe (001) and (100) crystal planes with the spacing distances of about 0.701 and 0.372 nm, respectively, can be seen along and perpendicular to

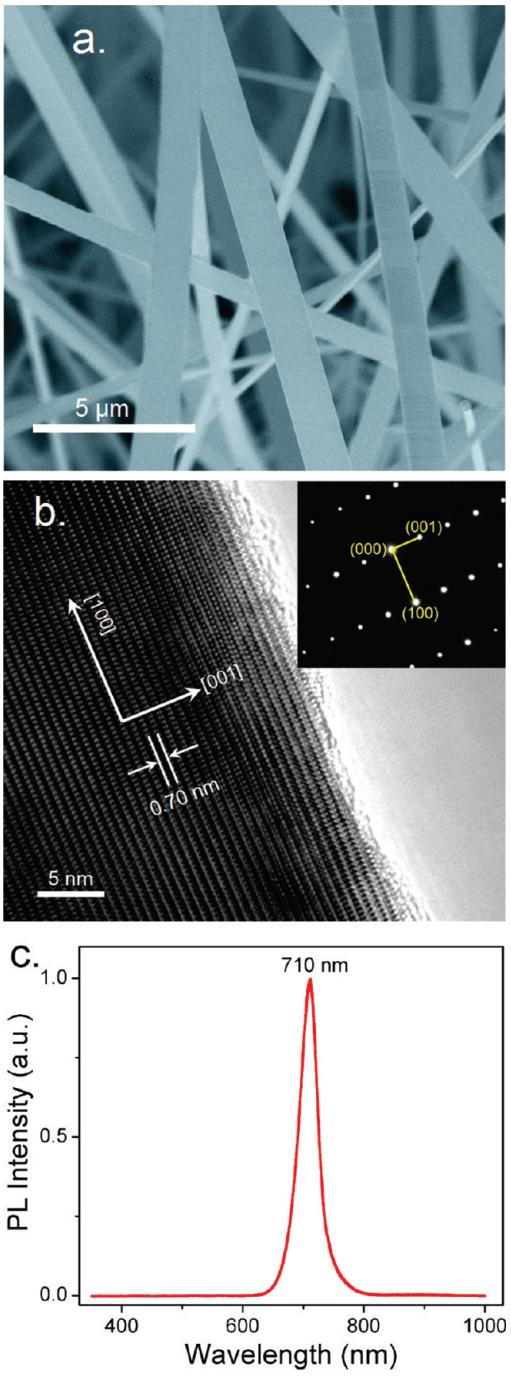

Figure 1. (a) Typical FESEM image of the CdSe NBs. (b) Typical HRTEM image together with the SAED pattern of a CdSe NB. (c) Typical room-temperature PL spectrum of a CdSe NB.

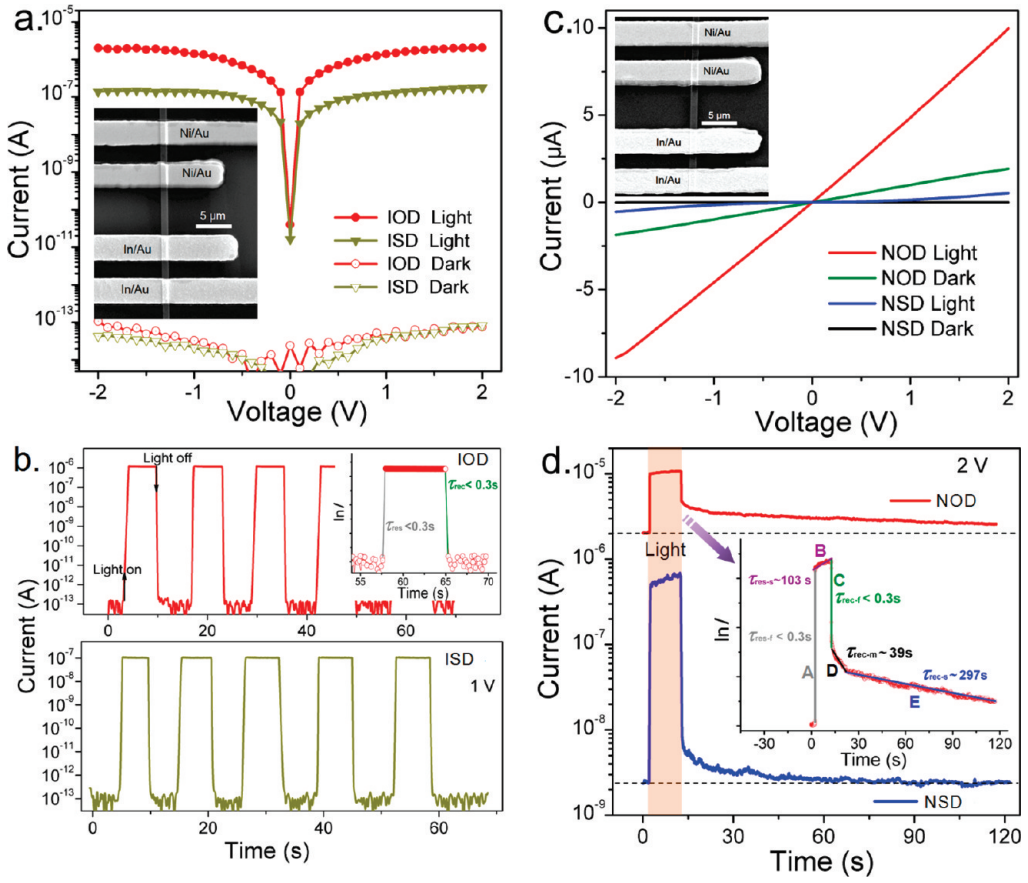

Figure 2. (a) Typical $I-V$ relations of a IOD and a ISD in dark and under constant 633 nm light illumination (0.13 W/cm^2). The inset is an FESEM image of them. (b) Reproducible light on/off switching properties of the two devices. The inset is a natural logarithmic plot of the time response spectrum of IOD. (c) Typical $I-V$ relations of a NOD and a NSD in dark and under illumination (633 nm, 0.13 W/cm^2). The inset is an FESEM image of them. (d) Reproducible light on/off switching properties of the two devices. The inset is a natural logarithmic plot of the time response spectrum of NOD.

the growth direction, respectively. Typical room-temperature PL spectrum (Figure 1c) of a single CdSe NB reveals a strong near-bandedge emission centered around 710 nm (~1.74 eV). No defect related PL peak is found.

Figure 2a shows typical current versus voltage ($I-V$) relations for an IOD and an ISD in dark and under constant (0.13 W/cm^2) 633 nm light illumination. The symmetric curves suggest that the two electrodes are identical in contact type in the respective devices. The dark currents of both devices are extremely small, which are near to the background noise (tens of femtoamperes). Under same light intensity and bias voltage, the photocurrent of IOD is larger than that of ISD, because of the Schottky barrier built in the ISD. The photosensitivity, which is defined as $(I_{photo}-I_{dark})/I_{dark}$, can be achieved to be about 5×10^7 in IOD at 1 V. To the best of our knowledge, this may be the highest reported value for semiconductor NS PDs. The inset of Figure 2a is an FESEM image of the devices. Herein, the width and thickness of the NB are about 973 and 87 nm, respectively. The gap between the two In/Au (two Ni/Au) electrodes is about 2.47 μm (2.43 μm). The electron concentration of the *i*-CdSe NB in dark can be estimated to be 1×10^9 cm^{-3}. The photoconductive gain (G), defined as the number of charges collected by electrodes due to excitation by one photon, is a key parameter to evaluate the sensitivity of photodetectors. The gain can be expressed as $G = (\Delta I/P)(h\nu/q)$, where ΔI is the photocurrent ($\Delta I = I_{photo} - I_{dark}$), P is the light power absorbed by the effective conductive channel, $h\nu$ is the energy of an incident photon, q is the electron charge. By using the area of the effective NB conductive channel (973 nm $\times$2.47 μm (2.43 μm)), we can calculate the gains of the IOD and ISD to be about 1267 and 112, respectively, at 2 V. Figure 2b exhibits the reproducible light on/off switching properties upon 633 nm illumination (0.13 W/cm^2) measured with Keithley 4200. It is clear that both IOD and ISD are with excellent stability and reproducibility, as well as fast response and recovery speeds. The inset is a natural logarithmic plot of the rising and falling edges of the photoresponse of the IOD. Limited by the time response of the measurement apparatus (Keithley 4200), herein, we can not obtain accurately the response and recovery time constants τ_{res} (τ_{rec}) by fitting the rising and falling edges with equations $I = 1 - \exp(-t/\tau_{res})$ and $I = \exp(-t/\tau_{rec})$, respectively.[6,7,15,31] However, it is certain that both τ_{res} and τ_{rec} are shorter than 0.3 s. Besides, it is clear that we can obtain the photosensitivities of ~1×10^7 and ~1×10^6 in the IOD and ISD, respectively, within 0.3 s.

Figure 2c shows typical $I-V$ relations of a NOD and a NSD in dark and under constant (0.13 W/cm^2) 633 nm light illumination. The width and thickness of the NB (inset of Figure 2c) are about 960 and 81 nm, respectively. The gap (L) between the two In/Au (two Ni/Au) electrodes is about 2.19 μm (2.25 μm). The resistivity (ρ) of the *n*-CdSe NB in dark can be calculated to be about 3.5 Ω cm with the equation $\rho = RS/L$, where R is the resistance (~1 MΩ) and S is cross-sectional area (960 $\times$ 81 nm^2). Assuming a mobility (μ_e) value of the CdSe NB to

dx.doi.org/10.1021/am200043c |ACS Appl. Mater. Interfaces 2011, 3, 1859–1864

be ~100 $cm^2/(V\,s)$, we can estimated the electron concentration to be about 1.8×10^{16} cm^{-3} with the equation $n = 1/(\rho e \mu_e)$. The photosensitivities of NOD and NSD are about 4 and 200, respectively, at 2 V. Compared with NOD, there is an enhanced photosensitivity in NSD. Because the Schottky barriers has remarkably reduced the dark current in NSD.[11−13] The photoconductive gains of NOD and NSD at 2 V are about 5803 and 407, respectively. Each value is about five times higher than that of the corresponding *i*-CdSe NB PDs. Figure 2d exhibits the light on/off switching properties of the NOD and NSD upon 633 nm illumination (0.13 W/cm^2) measured with Keithley 4200. We can see that the recovery process of NSD is faster than that of NOD, which again benefits from the gating effect of the Schottky barriers. The rising and falling edges of the photoresponse of NOD are shown in the inset of Figure 2d. Herein, by fitting the rising edges with equation $I = 1- \exp(-t/\tau_{res})$, we can obtain two time constants: $\tau_{res\text{-}f}$ (<0.3 s) and $\tau_{res\text{-}s}$(~103 s), corresponding to the fast (A) and slow (B) response processes, respectively. Analogously, by fitting the falling edges with equation $I = \exp(-t/\tau_{rec})$, we can obtain three time constants $\tau_{rec\text{-}f}$ (<0.3 s), $\tau_{res\text{-}m}$ (~39 s), and $\tau_{res\text{-}s}$ (~297 s), corresponding to the fast (C), medium (D),and slow (E) recovery processes, respectively. The fast processes (A and C) arise from the fast carrier photogeneration (recombination). The different time constants in slow (B, E) and medium processes (D) imply the existence of various traps in the *n*-CdSe NB. We have further investigated the relevance of the Schottky barrier to the photoresponse by studying the photoresponse properties of *n*-CdSe NB PDs with different Schottky barriers. We found that the device with higher Schottky barrier height (SBH) and/or thicker Schottky barrier (SBW) width would possess higher recovery speed but smaller photocurrent under the same condition. These phenomena can be understood as follow: under the same illumination, the effects of SBH lowering and SBW thinning are weaker in PDs with higher SBH and thicker SBW, and thus more difficult electron crossing and tunneling would happen in them. When the light is turned off, the recovery of SBH and SBW enables less current flowing through the device.

Compared with *i*-CdSe NB PDs, the photocurrents and gains of the *n*-CdSe NB PDs are much larger, whereas the response and recovery speeds of them are much lower. These results can be understood as follows: There exist various traps in semiconductor PDs, which would trap the photogenerated minority carriers (i.e., the photogenerated minority carrier lifetime would be prolonged), leaving behind unpaired majority carriers and resulting in an enhanced photocurrent. Generally speaking, there are two types of traps existing in semiconductor, one type originates from the surface states, i.e., from the surface defects, dangling bonds, adsorbates, etc.; the other originates from the impurity/defect states inside semiconductor.[6,7,15] In our experiment, because the sizes of the *i*- and *n*- CdSe NBs employed are nearly identical, the light power absorbed by the effective conductive channel under the same light intensity should be nearly the same. Lee et al.[15] have found that the conductance of the SiO_2-coated CdSe NB, either in dark or with light irradiation, dramatically increased compared to those before coating. On the other hand, the response speed of the coated nanoribbon clearly decreases. Based on these observations, they thought that surface defects and adsorbents serve mainly as recombination centers while not trapping centers for CdSe. Therefore, we think the main reason accounting for the lower recovery speed and higher photocurrent of the *n*-CdSe NB PDs is the carrier trapping

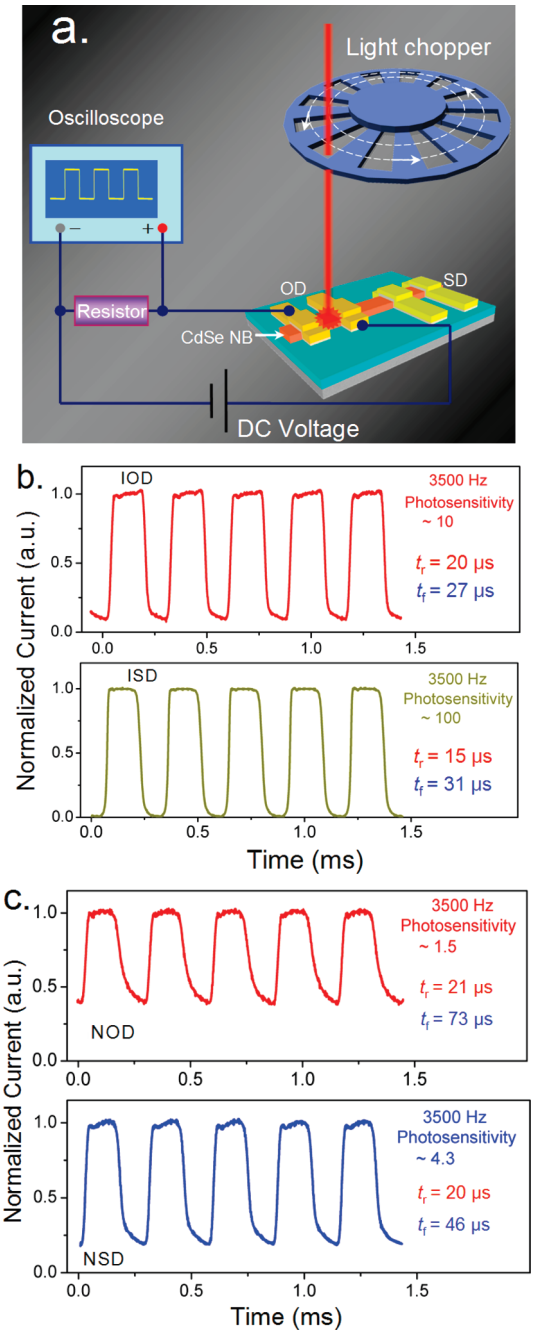

Figure 3. (a) Schematic diagram of our experimental setup for investigating the photoresponse speed of the CdSe NB PDs. (b, c) High-speed photoresponse properties of the PDs made from an individual *i*-CdSe NB and an individual *n*-CdSe NB, respectively. The light intensity is about 1.3 W/cm^2 and the bias voltage is 5 V.

centers due to impurity inside the *n*-CdSe NB. In addition, the Fermi level in *n*-CdSe NB is higher than that in *i*-CdSe NB, which will benefit better ohmic contacts for NOD and enhance the photocurrent for NSD under same light intensity.

Speed is a key parameter of PD, which describes the capability of a PD to follow fast-varying optical signals. Figure 3a is the schematic diagram of our experiment setup for studying the detailed photoresponse speed of the NB PDs. In this setup, a mechanical light chopper was used to turn the 633 nm He−Ne laser (~1.3 W/cm^2), and an oscilloscope was used to monitor

Table 1. Summary of the Photoresponse Properties of the PDs Studied in This Work

device[a]	photosensi-tivity[b]	responsivity (A/W)[c]	gain[d]	response time (μs)[e]	recovery time (μs)[e]	device size[f]
IOD	10 to 5 × 10^7	3060	6600	20	27	2.47 μm (gap) × 973 nm (w) × 87 nm (h)
ISD	100 to 1 × 10^7	240	470	15	31	2.43 μm (gap) × 973 nm (w) × 87 nm (h)
NOD	1.5−4	1.5 × 10^4	3 × 10^4	21	73	2.19 μm (gap) × 960 nm (w) × 81 nm (h)
NSD	4.3−200	1020	2 × 10^3	20	46	2.25 μm (gap) × 960 nm (w) × 81 nm (h)

[a] All the measurements were carried out at room temperature in air. [b] Photosensitivity = $\Delta I/I_{dark}$. [c] Responsivity = $\Delta I/P$. [d] Gain = $(\Delta I/P)(h\nu/q)$ is also known as photoconductive gain, external quantum efficiency, or quantum efficiency. [e] Response time is defined as the time required for photocurrent to increase from 10% I_{peak} to 90% I_{peak}, and Recovery time is defined analogously. [f] (gap), (w) and (h) stand for electrode separation, width, and thickness of the NB, respectively.

the time dependence of the photocurrent. The impedance was 1 kΩ. Figure 3b displays the photoresponse properties of the *i*-CdSe NB PDs under a 3500 Hz pulsed illumination. The bias voltage is 5 V. The measured response time (i.e., rise time t_r), defined as the time required for photocurrent to increase from 10% to 90% I_{peak},[25] and the recovery time (i.e., fall time t_f), defined analogously, are 20 and 27 μs for IOD, and 15 and 31 μs for ISD, respectively. The corresponding photosensitivties are about 10 and 100 for IOD and ISD, respectively. Here, the higher photosensitivity in ISD again results from the Schottky barriers induced lower dark current. In addition, unlike the results under illumination with low switching frequency (Figure 2b), the dark currents here can not return back to near-zero. This suggests the existence of some traps in the *i*-CdSe NB. Figure 3c displays the high-speed photoresponse properties of the *n*-CdSe NB PDs. The measured response and recovery times t_r/t_f are about 21/73 μs for NOD, and 20/46 μs for NSD, respectively. The photosensitivties are about 1.5 and 4.3 for NOD and NSD, respectively. Here, the smaller photosensitivity (∼1.5) and longer recovery time (∼73 μs) for NOD compared with the corresponding values for IOD (10 and 27 μs, respectively), confirm once again that there are more impurity induced traps inside the *n*-CdSe NB.

It is worth noting that, for practical applications, the achievement of fast speed and simultaneous high photosensitivity is highly desired.[31] Table 1 is the summary of the photoresponse properties of the CdSe NB PDs studied in this work. We can see that, under a 3500 Hz pulsed illumination, all the four types of PDs can exhibit high response speeds (∼20 μs) and a photosensitivity more than unity simultaneously. Particularly, the obtained short response/recovery times of 15/31 μs and a simultaneous high photosensitivity of 100 in ISD may be the best result reported so far, to the best of our knowledge, in the effort of getting fast speed and high photosensitivity simultaneously in semiconductor NS PDs.[31] Moreover, from Table 1, it is clear that the *i*-CdSe NBs are more suitable for fast and sensitive photodetecting applications, while extrinsic *n*-CdSe NBs are more advantageous for high-gain PDs. This conclusion can be applicable to other semiconductor nanomaterials.[6,34−36] Besides, our results confirm that Schottky contact-based PDs show higher speeds compared with the ohmic contact-based PDs, whereas the ohmic contact-based PDs possess higher gain in return.

CONCLUSIONS

In summary, we have investigated the impurity-dependent photoresponse properties of single CdSe NBs, with the case of both ohmic and Schottky contact based PDs made from individual *i*- and *n*-CdSe NBs. The sizes of the *i*- and *n*- NBs were purposely chosen to be nearly identical to minimize the size-dependent effect. We found that *i*-CdSe NB PDs possess higher photosensitivities and higher speeds than *n*-CdSe NB PDs in a wide range of switching frequency (up to 3500 Hz), while the *n*-CdSe NB PDs show larger photoconductive gains in return. We have concluded that the different photoresponse properties resulted mainly from the impurity induced traps. This conclusion can be applicable to other semiconductor nanomaterials. Moreover, we have achieved the short response/recovery times of 15/31 μs and a simultaneous high photosensitivity of 100 from ISD under a 3500 Hz illumination. This may be the best reported result so far in the effort of getting a fast speed and a high photosensitivity simultaneously for practical PD applications.

AUTHOR INFORMATION

Corresponding Author
*E-mail: lundai@pku.edu.cn.

ACKNOWLEDGMENT

This work was supported by the National Natural Science Foundation of China (10774007, 11074006, 10874011, 50732001), the National Basic Research Program of China (2006CB921607, 2007CB613402), and the Scholarship Award for Excellent Doctoral Student granted by Ministry of Education.

REFERENCES

(1) Wang, J.; Gudiksen, M. S.; Duan, X.; Cui, Y.; Lieber, C. M. *Science* **2001**, *293*, 1455–1457.
(2) Kind, H.; Yan, H.; Messer, B.; Law, M.; Yang, P. *Adv. Mater.* **2002**, *14*, 158–160.
(3) Freitag, M; Martin, Y.; Misewich, J. A.; Martel, R.; Avouris, Ph. *Nano Lett.* **2003**, *3*, 1067–1071.
(4) Calarco, R.; Marso, M.; Richter, T.; Aykanat, A. I.; Meijers, R.; Hart, A. v.d.; Stoica, T.; Lüth, H. *Nano Lett.* **2005**, *5*, 981–984.
(5) Hayden, O.; Agarwal, R.; Lieber, C. M. *Nat. Mater.* **2006**, *5*, 352–356.
(6) Jie, J. S.; Zhang, W. J.; Jiang, Y.; Meng, X. M.; Li, Y. Q.; Lee, S. T. *Nano Lett.* **2006**, *6*, 1887–1892.
(7) Soci, C.; Zhang, A.; Xiang, B.; Dayeh, S. A.; Aplin, D. P. R.; Park, J.; Bao, X. Y.; Lo, Y. H.; Wang, D. *Nano Lett.* **2007**, *7*, 1003–1009.
(8) Fan, Z.; Ho, J. C.; Jacobson, Z. A.; Razavi, H.; Javey, A. *Proc. Natl. Acad. Sci. U.S.A.* **2008**, *105*, 11066–11070.
(9) Yang, Q.; Guo, X.; Wang, W.; Zhang, Y.; Xu, S.; Lien, D. H.; Wang, Z. L. *ACS Nano* **2010**, *4*, 285–6291.
(10) Neamen, D. A. *An Introduction to Semiconductor Devices*: McGraw-Hill: New York, 2006, pp 605−608.
(11) Zhou, J.; Gu, Y.; Hu, Y.; Mai, W.; Yeh, P. H.; Bao, G.; Sood, A. K.; Polla, D. L.; Wang, Z. L. *Appl. Phys. Lett.* **2009**, *94*, 191103.
(12) Wei, T. Y.; Huang, C. T.; Hansen, B. J.; Lin, Y. F.; Chen, L. J.; Lu, S. Y.; Wang, Z. L. *Appl. Phys. Lett.* **2010**, *96*, 013508.
(13) Law, J. B. K.; Thong, J. T. L. *Appl. Phys. Lett.* **2006**, *88*, 133114.

(14) Yang, C.; Barrelet, C. J.; Capasso, F.; Lieber, C. M. *Nano Lett.* **2006**, *6*, 2929–2934.
(15) Jiang, Y.; Zhang, W. J.; Jie, J. S.; Meng, X. M.; Fan, X.; Lee, S. T. *Adv. Funct. Mater.* **2007**, *17*, 1795–1800.
(16) Lin, C. H.; Chen, T. T.; Chen, Y. F. *Opt. Express* **2008**, *16*, 16916–16922.
(17) Zhai, T.; Fang, X.; Liao, M.; Xu, X.; Zeng, H.; Bando, Y.; Golberg, D. *Sensors* **2009**, *9*, 6504–6529.
(18) Thunich, S.; Prechtel, L.; Spirkoska, D.; Abstreiter, G.; Morral, A. F. i; Holleitner, A. W. *Appl. Phys. Lett.* **2009**, *95*, 083111.
(19) Sahoo, S.; Husale, S.; Colwill, B.; Lu, T. M.; Nayak, S.; Ajayan, P. M. *ACS Nano* **2009**, *3*, 3935–3944.
(20) Zhai, T.; Ye, M.; Li, L.; Fang, X.; Liao, M.; Li, Y.; Koide, Y.; Bando, Y.; Golberg, D. *Adv. Mater.* **2010**, *22*, 4530–4533.
(21) Huang, K.; Zhang, Q.; Yang, F.; He, D. *Nano Res.* **2010**, *3*, 281–287.
(22) Zhai, T.; Li., L.; Wang, X.; Fang, X.; Bando, Y.; Golberg, D. *Adv. Funct. Mater.* **2010**, *20*, 4233–4248.
(23) Yoon, Y. J.; Park, K. S.; Heo, J. H.; Park, J. G.; Nahm, S.; Choi, K. J. *J. Mater. Chem.* **2010**, *20*, 2386–2390.
(24) Zhai, T.; Ma, Y.; Li, L.; Fang, X.; Liao, M.; Koide, Y.; Yao, J.; Bando, Y.; Golberg, D. *J. Mater. Chem.* **2010**, *20*, 6630–6637.
(25) Wu, P. C.; Dai, Y.; Ye, Y.; Yin, Y.; Dai, L. *J. Mater. Chem.* **2011**, *21*, 2563–2567.
(26) Zhai, T.; Fang, X.; Liao, M.; Xu, X.; Li, L.; Liu, B.; Koide, Y.; Ma, Y.; Yao, J.; Bando, Y.; Golberg, D. *ACS Nano* **2010**, *4*, 1596–1602.
(27) Yan, C.; Singh, N.; Cai, H.; Gan, C. L.; Lee, P. S. *ACS Appl. Mater. Interfaces* **2010**, *7*, 1794–1797.
(28) Rigutti, L.; Tchernycheva, M.; De Luna Bugallo, A.; Jacopin, G.; Julien, F. H.; Zagonel, L. F.; March, K.; Stephan, O.; Kociak, M.; Songmuang, R. *Nano Lett.* **2010**, *10*, 2939–2943.
(29) Gu, Y.; Kwak, E.-S.; Lensch, J. L.; Allen, J. E.; Odom, T. W.; Lauhon, L. J. *Appl. Phys. Lett.* **2005**, *87*, 043111.
(30) Chen, M. W.; Chen, C. Y.; Lien, D. H.; Ding, Y.; He, J. H. *Opt. Express* **2010**, *18*, 4836–14841.
(31) Kung, S. C.; Van der Veer, W. E.; Yang, F.; Donavan, K. C.; Penner, R. M. *Nano Lett.* **2010**, *10*, 1481–1485.
(32) Liu, C.; Wu, P. C.; Sun, T.; Dai, L.; Ye, Y.; Ma, R. M.; Qin, G. G. *J. Phys. Chem. C* **2009**, *113*, 14478–14481.
(33) Kim, C. J.; Lee, H. S.; Cho, Y. J.; Kang, K.; Jo, M. H. *Nano Lett.* **2010**, *10*, 2043–2048.
(34) Liu, Y.; Zhou, X.; Hou, D.; Wu, H. *J. Mater. Sci.* **2006**, *41*, 6492–6496.
(35) Li, L.; Wu, P. C.; Fang, S. H.; Zhai, T. Y.; Dai, L.; Liao, M. Y.; Koide, Y.; Wang, H. Q.; Bando, Y.; Golberg, D. *Adv. Mater.* **2010**, *22*, 3161–3165.
(36) Ye, Y.; Dai, L.; Wen, X.; Wu, P. C.; Pen, R. M.; Qin, G. G. *ACS Appl. Mater. Interfaces* **2010**, *2*, 2724–2727.